# Minkowski sum boundary surfaces of 3D-objects

Martin Peternell Tibor Steiner

January 15, 2007

Address: Institute of Discrete Mathematics and Geometry,
University of Technology Vienna,
Wiedner Hauptstraße 8–10,
1040 Wien,
Austria

| | |
|---|---|
| email: | peternell@geometrie.tuwien.ac.at |
| phone: | +43-1-58801-11313 |
| fax: | +43-1-58801-11399 |

**Abstract**

Given two objects $A$ and $B$ with piecewise smooth boundary we discuss the computation of the boundary $\Gamma$ of the *Minkowski sum* $A+B$. This boundary surface $\Gamma$ is part of the envelope when $B$ is moved by translations defined by vectors $\mathbf{a} \in A$, or vice versa. We present an efficient algorithm working for dense point clouds or for triangular meshes. Besides this the global self-intersections of the boundary $\Gamma$ are detected and resolved. Additionally we point to some relations between Minkowski sums and kinematics, and compute local quadratic approximations of the envelope.



*keywords:* Minkowski sum, convolution surface, translation, motion, envelope, marching algorithm, point-set surface, signed distance function.

# 1 Introduction

Minkowski sums in two and three dimensions are used in various fields, for example mathematical morphology, computer graphics, convex geometry and computational geometry. Given two sets $\mathcal{A}$ and $\mathcal{B}$, the set

$$\{\mathbf{a}+\mathcal{B}|\mathbf{a}\in\mathcal{A}\} = \{\mathbf{a}+\mathbf{b}|\mathbf{a}\in\mathcal{A},\mathbf{b}\in\mathcal{B}\} = \mathcal{A}+\mathcal{B} \tag{1}$$

is called the *Minkowski sum* $\mathcal{A}+\mathcal{B}$ of the sets $\mathcal{A},\mathcal{B}$. It is formed by translating the set $\mathcal{B}$ by all vectors $\mathbf{a}\in\mathcal{A}$, and it is obvious that the sets $\mathcal{A}$ and $\mathcal{B}$ can be exchanged. The definition does not require any smoothness, but later on we will concentrate on sets $\mathcal{A},\mathcal{B}$ with piecewise smooth boundaries $\partial\mathcal{A}$ and $\partial\mathcal{B}$.

The boundary $\partial(\mathcal{A}+\mathcal{B})$ of the Minkowski sum A+B is contained in the *envelope* of $\mathcal{B}$ with respect to the translations $\mathbf{x}'=\mathbf{a}+\mathbf{x}$, $\mathbf{a}\in\mathcal{A}$. Since we prefer to use boundary representations for geometric objects, the Minkowski sum will be represented by its boundary surface, too. It is sufficient to apply translations defined by vectors $\mathbf{a}\in\partial\mathcal{A}$ to the boundary points of $\mathcal{B}$. When studying envelopes it is not necessary that the input objects are solids but can be surfaces as well.

Applying the concept of Minkowski sum to surfaces $A$ and $B$ may cause some confusion since the surfaces are already boundaries (not necessarily closed). Figure 1 illustrates the 2D-case for two planar curves $A,B$ bounding planar domains $\mathcal{A},\mathcal{B}$. The set $A+B$ is covered by two families of curves $\mathbf{a}+B$ and $\mathbf{b}+A$. The family $\mathbf{a}+B$ consists of congruent curves translating $B$ when $\mathbf{a}$ varies in $A$. Analogously $A+B$ is covered by $\mathbf{b}+A$ for a moving point $\mathbf{b}\in B$. These two families of curves possess an *envelope* called the *convolution* $A\star B$ of $A$ and $B$. It might consist of several components. The outer boundary $\Gamma$ of the envelope $A\star B$ is the boundary $\partial(\mathcal{A}+\mathcal{B})$ of the Minkowski sum $\mathcal{A}+\mathcal{B}$ of the sets $\mathcal{A},\mathcal{B}$. In many applications $A$ and $B$ are oriented surfaces which implies that $A\star B$ is an oriented envelope. The outer boundary $\Gamma$ is the trimmed outer component of $A\star B$.

In order to guard against misunderstandings we note that convolution surfaces appear in computer graphics and visualization also in a different way, see e.g. [2, 11, 18]. There, a convolution surface is defined as level set of an implicit function $f(\mathbf{x}) = g(\mathbf{x})\star h(\mathbf{x}) = \int_{\mathbb{R}^3} g(\mathbf{t})h(\mathbf{x}-\mathbf{t})d\mathbf{t}$, called the convolution of the *geometry function* $g$ and the *kernel function* $h$.

There exist several contributions concerning the analysis of algorithms and the computation

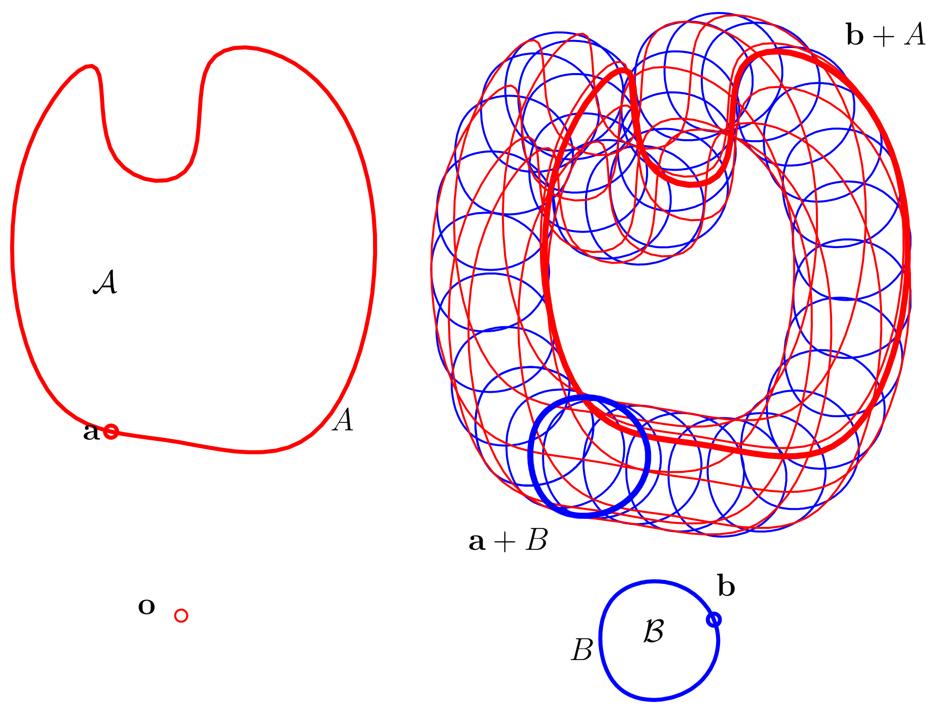


Figure 1: Construction of two families of curves $\mathbf{a} + B$ and $\mathbf{b} + A$

of Minkowski sums. In particular the 2D case is investigated thoroughly, for polygons as well as for smooth curves, see for instance [4, 6, 7, 8, 9].

The computation of the Minkowski sum of two convex objects is well known, see e.g. [12]. The handling of the non-convex case is thus often solved by decomposing the input polytopes into convex components, see e.g. [5]. The Minkowski sum of two non-convex objects is thus obtained by computing the Minkowski sums of all pairs of convex parts. Finally these partial Minkowski sums have to be glued together. In [19] this concept is applied to the Minkowski sum computation of complex polyhedral objects.

When dealing with *boundary representations* of geometric objects, the computation of the envelope with respect to translations is advantageous, since the convex decomposition of free-form input geometries results in a large number of convex parts. Thus the union of a large number of partial Minkowski sums is the challenging part of a practical implementation.

If the input objects are represented by their boundaries, there are mainly two cases: The objects are given explicitly by parametric representations or by a piecewise planar approximation, consisting of triangular or polygonal faces. In general, the Minkowski sum computation with respect to parametric representations of the input objects results in a difficult reparametrization problem and is in close relation to the convolution of two surfaces, see [8, 10, 13, 16, 17].

The aim of this contribution is twofold. On the one hand we present a method to compute the Minkowski sum of two objects $\mathcal{A}, \mathcal{B}$ with piecewise smooth boundary surfaces $A = \partial\mathcal{A}$, $B = \partial\mathcal{B}$, which are assumed to be given by dense clouds of data points in order to estimate surface normals and second order properties. On the other hand a local analysis of the envelope $A \star B$ is performed. A detailed investigation of doubly curved input surfaces shows how the regularity of the convolution depends on the relation of the normal curvatures of $A$ and $B$.

The Minkowski sum computation follows the following concept:

- Computation of the envelope $A \star B$.
- Extraction of the outer boundary $\Gamma$ (and possibly inner boundaries) of the envelope.
- Treatment of global self-intersections.
- Triangulation of the final point set.

Assuming that the boundary surfaces $A, B$ are defined by points $\mathbf{a}, \mathbf{b}$ plus oriented unit normal vectors $\mathbf{n}_a, \mathbf{n}_b$, the same description will be available for the envelope $A \star B$ and its outer boundary $\Gamma$. The extraction of the outer boundary $\Gamma$ is performed by a marching method in the distance field of the envelope. This is a standard method for trimming, see[20] and results in fact in a discretized implicit representation of the Minkowski sum. A similar method can be applied to extract possibly occurring inner boundaries of the envelope. The global self-intersections of $\Gamma$ can be detected with relatively high reliability by investigating the variation of the normal vectors at points of $\Gamma$. The test examples (figures 6, 7, 9, 10) show that the presented method works with high precision and yields reliable results.

The article is organized as follows. Section 2 provides an introduction to convolution surfaces and envelope computation. The case of parametric input surfaces as well as the local quadratic approximations are briefly discussed in Section 3. Section 4 tells about convolution of point clouds, extraction of the outer boundary and the detection of self-intersections. Finally we conclude the paper in section 5.

# 2 Geometric background

Let $\mathcal{A}, \mathcal{B}$ be two objects in space with piecewise smooth boundary surfaces $A = \partial\mathcal{A}$, $B = \partial\mathcal{B}$. We discuss the construction of the convolution surface $A \star B$ and its main geometric properties.

## 2.1 Convolution of two surfaces

A (local) parametrization $\mathbf{a}(u, v)$ of the input surface $A$ defines a two-parameter family of translations $\mathbf{x}' = \mathbf{a}(u, v) + \mathbf{x}$. At any smooth position there exist linearly independent partial derivative vectors

$$\mathbf{a}_u = \frac{\partial \mathbf{a}}{\partial u}, \mathbf{a}_v = \frac{\partial \mathbf{a}}{\partial v}.$$

Let $\mathbf{a}(t) = \mathbf{a}(u(t), v(t))$ be a curve in $A$ and $\mathbf{x}' = \mathbf{a}(t) + \mathbf{x}$ be the corresponding one-parameter family of translations. The velocity vector field $\mathbf{v}(t) = \dot{\mathbf{a}}(t) = \mathbf{a}_u u_t + \mathbf{a}_v v_t$ is independent of the point $\mathbf{x}$.

Since we are interested in boundary representations we do not apply all translations $\mathbf{a} \in A$ to all points $\mathbf{b} \in B$ but we are looking for those pairs of points $\mathbf{a}, \mathbf{b}$ such that $\mathbf{a} + \mathbf{b}$ is a boundary point of the envelope of the two-parameter family of surfaces $\mathbf{a} + B$. For the given motion $\mathbf{x}' = \mathbf{a}(u, v) + \mathbf{x}$ only those points $\mathbf{b} \in B$ will contribute to the envelope, if both $\mathbf{a}_u$ and $\mathbf{a}_v$ are tangent to the surface $B$ at $\mathbf{b}$. This in fact requires smoothness of the input surfaces $A$ and $B$. In other words, $\mathbf{a} + \mathbf{b}$ is a point of the envelope if the tangent planes $T_a$ and $T_b$ at points $\mathbf{a}, \mathbf{b}$ are parallel. Since we assume that $A, B$ are oriented surfaces it is more precise to formulate a condition involving oriented unit normal vectors $\mathbf{n}_a, \mathbf{n}_b$ of $A, B$. This leads to the notion of *convolution surfaces* which are defined in the following way:

Given two oriented smooth surfaces $A$ and $B$ with unit normal vectors $\mathbf{n}_a$ $\mathbf{n}_b$, the convolution surface $A \star B$ is defined by

$$A \star B = \{\mathbf{a} + \mathbf{b} | \mathbf{n}_a = \mathbf{n}_b, \mathbf{a} \in A, \mathbf{b} \in B\}. \tag{2}$$

Since $A \star B$ is defined with respect to orientations of the normal vectors, it is an *oriented envelope*. If $A, B$ are smooth boundaries of sets $\mathcal{A}, \mathcal{B}$, the boundary of the Minkowski sum $\partial(\mathcal{A}+\mathcal{B})$ is usually a subset of the convolution $A \star B$. To figure out which points of $A \star B$ are in fact boundary points of the Minkowski sum $\mathcal{A}+\mathcal{B}$, a trimming of the convolution $A \star B$ is performed, see Figure 5.

## 2.2 Convolution of a surface and a curve

One can generalize the concept of Minkowski sum and convolution surfaces to the case where $A$ is a smooth curve and $B$ is a piecewise smooth surface in a straightforward manner. Let the curve $A$ be parametrized by $\mathbf{a}(t)$, the convolution is defined by

$$C = A \star B = \{\mathbf{a}+\mathbf{b} | \dot{\mathbf{a}} \cdot \mathbf{n}_b = 0,\ \mathbf{a} \in A, \mathbf{b} \in B\}. \tag{3}$$

The vector sum is formed for those pairs of points $\mathbf{a}, \mathbf{b}$ where the tangent vector $\dot{\mathbf{a}}$ is parallel to the tangent plane of $\mathbf{b}$. This definition is equivalent to (2).

The convolution is the envelope of $B$ with respect to a one-parameter family of motions $\mathbf{x}' = \mathbf{a}(t) + \mathbf{x}$. Thus, the computation of the convolution of a curve and a surface is simpler than for two surfaces. This concept applies to the convolution of a surface and a pipe surface which can be considered as offset of its center curve. Moreover it is useful when computing convolution surfaces of piecewise smooth objects which possess sharp edges, see Section 4.4.

# 3 Computing the envelope for parametrized surfaces

We are given two smooth oriented surfaces $A, B \subset \mathbb{R}^3$ by parametric representations

$$\mathbf{a}(u,v) : G \subset \mathbb{R}^2 \to A, \quad \mathbf{b}(s,t) : H \subset \mathbb{R}^2 \to B,$$

where $G$ and $H$ are planar domains in $\mathbb{R}^2$. The unit normal vectors of $A, B$ are denoted by $\mathbf{n}_a(u,v)$ and $\mathbf{n}_b(s,t)$, but their normalization is not essential. In order to compute the envelope of $B$ with respect to translations defined by $\mathbf{a}$, or equivalently, the convolution surface $A \star B$, we have to construct a reparametrization

$$\begin{aligned} \phi : H &\to G, \\ (s,t) &\mapsto (u,v) \end{aligned}$$

such that $\mathbf{n}_a(\phi(s,t)) = \mathbf{n}_b(s,t)$ holds. The mapping $\phi$ is assumed to be a *local diffeomorphism*, but in general it is not one-to-one. Under the assumption that we have already found a reparametrization $\phi$, the envelope $A \star B$ is parametrized by

$$\mathbf{c}(s,t) = \mathbf{a}(\phi(s,t)) + \mathbf{b}(s,t).$$

In particular cases there exist explicit parametrizations of the convolution of two surfaces. We mention that the *convolution of two spheres* is a sphere, which is geometrically evident, since if the center of a sphere moves along another sphere, the envelope is again a sphere. An analogous result holds for two paraboloids with parallel axes, see section 3.1.

Further it is shown in [13] that the convolution of an arbitrary rational surface and a paraboloid is again a rational surface, and the reparametrization can be given explicitly. The same property holds for a larger class of surfaces, whose normal vectors admit a linear parametrization in the surface parameters, see [16]. In this sense, these surfaces are generalizations of paraboloids. Convolution surfaces of two ruled surfaces can also be parametrized explicitly, see [10]. Similar properties hold for two canal surfaces. The existence of explicit parametrizations is in close relation to the structure of the normal vector fields of the input surfaces.

Moreover we point to some *degenerate cases* concerning the unit normal vector field of the input surfaces. Let $A$ be planar, then $\mathbf{n}_a$ is a constant vector. Assume that $\mathbf{n}_b(s,t)$ is an injective parametrization of a part of the unit sphere $S^2$, then there exists at most a single point $\mathbf{b}_0 = \mathbf{b}(s,t)$ whose normal vector satisfies $\mathbf{n}_b(s,t) = \mathbf{n}_a$. In other words, $\mathbf{b}_0$ corresponds to all points $\mathbf{a} \in A$. We conclude that $A \star B$ is planar with $\mathbf{a}(u,v) + \mathbf{b}_0$ as possible parametrization.

Let $A$ be a developable surface, then $\mathbf{n}_a(u,v)$ is a curve in $S^2$. Without loss of generality we assume that this curve is parametrized by $\mathbf{n}_a(u)$. This says in particular that $\mathbf{a}(u_0,v)$ parametrizes a generating line in $A$ for fixed $u_0$. If $\mathbf{n}_b(s,t)$ is injective, there exists in general a curve $\mathbf{b}(s(u),t(u))$ which contributes to the construction. Since all points $\mathbf{a}(u_0,v)$ correspond to a single point $\mathbf{b}(s(u_0),t(u_0))$, the sum $\mathbf{a}(u_0,v)+\mathbf{b}(s(u_0),t(u_0))$ is a generating line in $A \star B$. Points on this line possess unit normals $\mathbf{n}_a(u_0)$. Since this property holds for all $(u,v) \in G$, the envelope $A \star B$ is a developable surface.

### Convolution surfaces of translated input objects

For practical considerations it is remarkable that *the convolution $A \star B$ is invariant with respect to translations* in the following sense: Let $\tau : \mathbf{x}' = \mathbf{v} + \mathbf{x}$ be a fixed translation, and let $B' = \tau(B)$. Thus, $B'$ admits the parametrization $\mathbf{b}'(s,t) = \mathbf{b}(s,t) + \mathbf{v}$. We assume that $\mathbf{a}(\phi(s,t))$ is already a parametrization of $A$ with respect to coinciding unit normals $\mathbf{n}_a(\phi(s,t)) = \mathbf{n}_b(s,t)$. Because $\mathbf{b}(s,t)$ and $\mathbf{b}'(s,t)$ possess the same unit normal vectors $\mathbf{n}_b$, the convolution $A \star B'$ is parametrized by

$$\mathbf{a} + \mathbf{b}' = \mathbf{a} + \mathbf{b} + \mathbf{v} = \mathbf{c} + \mathbf{v}.$$

Thus, the convolution surface $A \star B'$ of $A$ and $B'$ is obtained by applying the translation $\tau$ to the convolution surface $C = A \star B$ of $A$ and $B$.

### Convolution surfaces of offsets of the input objects

Let $A$ and $B$ be two smooth oriented surfaces and let us assume that the reparametrization with respect to coinciding unit normal vectors $\mathbf{n}_a = \mathbf{n}_b$ has been performed already. Let $A$ and $B$ be parametrized by $\mathbf{a}(s,t)$ and $\mathbf{b}(s,t)$, respectively.

How does the convolution surface look like, if we replace $B$ by a one-sided offset $B_d$ at oriented distance $d$. In fact, $B$ and $B_d$ have the same unit normals $\mathbf{n}_b$, since $\mathbf{b}_d(s,t) = \mathbf{b}(s,t) + d\mathbf{n}_b(s,t)$. Since the unit normals of $B, B_d$ and $C$ coincide, we denote them by $\mathbf{n}$. As a direct consequence, the convolution $C' = A \star B_d$ is an *offset* of $C = A \star B$ at distance $d$, and a parametrization of $C'$ is obtained by

$$\mathbf{c}' = \mathbf{a} + \mathbf{b}_d = \mathbf{a} + \mathbf{b} + d\mathbf{n} = \mathbf{c} + d\mathbf{n}.$$

*Example*: Let $A$ be a piecewise smooth object and $B$ be a *pipe surface* with *spine curve* $M$ and radius $d$. The pipe surface $B$ itself is the envelope of a one-parameter family of spheres traveling along $M$. We interpret $M$ as offset of $B$ at distance $-d$, and the unit normals $\mathbf{n}_b$ of $B$ are perpendicular to $M$ (for corresponding parameter values). Thus, the convolution $C = A \star B$ is the offset of $C' = A \star M$ at oriented distance $d$.

### 3.1 Convolution surfaces of spheres and paraboloids and the quadratic approximation of general convolution surfaces

To get more insight into the computation of convolution surfaces, we discuss the convolution of two spheres and two paraboloids with parallel axes. Latter is a special case of the quadratic approximation of the convolution surface of two arbitrary analytic input surfaces. Figure 2 is an illustration of the planar case, showing the convolution of two circles and two parabolas with parallel axes.

#### Convolution of spheres

Let $A$ and $B$ be two oriented spheres with centers $\mathbf{r}$ and $\mathbf{s}$. Their signed radii are denoted by $r$ and $s$, and determine the orientation of $A$ and $B$. The convolution $C = A \star B$ is again a sphere, with center $\mathbf{r}+\mathbf{s}$ and radius $r+s$. This can be checked by using standard parametrizations

$$\mathbf{a}(u,v) = \mathbf{r} + r\mathbf{n}(u,v), \mathbf{b}(u,v) = \mathbf{s} + s\mathbf{n}(u,v)$$

for both $A$ and $B$, where $\mathbf{n}(u,v)$ is a parametrization of the unit sphere. Since the correspondence between $A$ and $B$ is defined by equal surface parameters $(u,v)$, the convolution surface $A \star B$ is parametrized by

$$\mathbf{c}(u,v) = \mathbf{a}(u,v) + \mathbf{b}(u,v) = \mathbf{r} + \mathbf{s} + (r+s)\mathbf{n}(u,v). \tag{4}$$

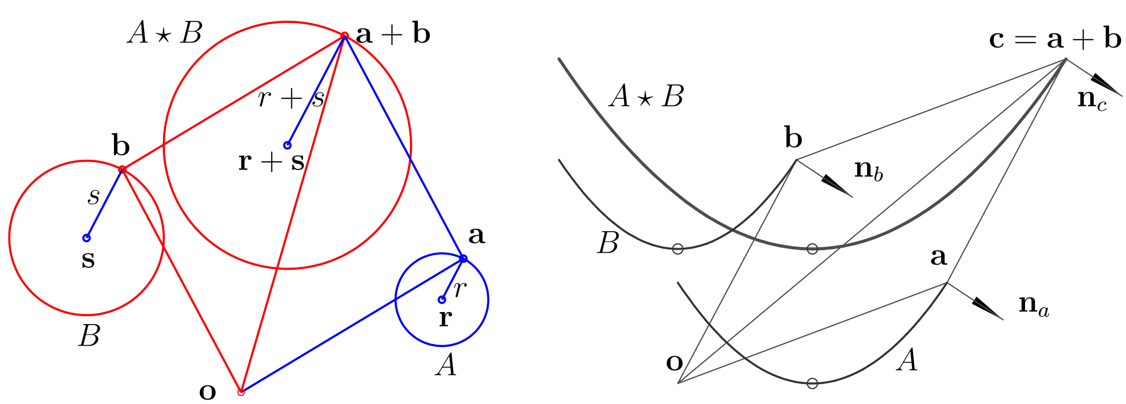


Figure 2: Convolution of two circles and two parabolas

**Quadratic approximation of the convolution surface of two smooth surfaces**

The computation of convolution surfaces is based on a simple operation, the sum of vectors, and the question arises how local approximations of convolution surfaces look like. As a byproduct of this investigation we obtain the result that the convolution of two paraboloids with parallel axis is again a paraboloid.

Let $A, B$ be two analytic surfaces. We assume that the regular points $\mathbf{a}_0, \mathbf{b}_0$ are a pair of corresponding points of $A, B$ with respect to coinciding unit normals. By applying a translation one achieves $\mathbf{a}_0 = \mathbf{b}_0$. We choose a coordinate system with $\mathbf{a}_0$ as origin and in a way that $A$ and $B$ are locally parametrized by the following graph representations,

$$\mathbf{a}(u,v) = (u, v, \frac{1}{2}(au^2 + cv^2) + O(x^3))^\top, \mathbf{b}(s,t) = (s, t, \frac{1}{2}(\alpha s^2 + 2\beta st + \gamma t^2) + O(x^3))^\top. \quad (5)$$

The third coordinates $a_3, b_3$ of $\mathbf{a}$ and $\mathbf{b}$ are expanded into Taylor–series and we do not take care of third or higher order terms. In order to obtain a compact and concise notation, we let $U = (u,v)^\top$ and $S = (s,t)^\top$, and set

$$D = \begin{bmatrix} a & 0 \\ 0 & c \end{bmatrix}, \text{ and } E = \begin{bmatrix} \alpha & \beta \\ \beta & \gamma \end{bmatrix}.$$

By the use of these abbreviations, the local parametrizations of $A, B$ are given by

$$\mathbf{a}(U) = \begin{bmatrix} U \\ \frac{1}{2}U^\top \cdot D \cdot U + O(x^3) \end{bmatrix}, \text{ and } \mathbf{b}(S) = \begin{bmatrix} S \\ \frac{1}{2}S^\top \cdot E \cdot S + O(x^3) \end{bmatrix}. \quad (6)$$

Since the gradients of the third coordinates $a_3, b_3$ of $\mathbf{a}, \mathbf{b}$ equal $\nabla a_3 = D \cdot U + O(x^2)$ and $\nabla b_3 = E \cdot S + O(x^2)$, the reparametrization $\phi$ and its inverse according to coinciding unit normals are given by

$$\phi : S \longrightarrow U = D^{-1} \cdot E \cdot S + O(x^2), \quad \phi^{-1} : U \longrightarrow S = E^{-1} \cdot D \cdot U + O(x^2). \quad (7)$$

These transformations require regularity of $D$ (or $E$), respectively, which is assumed in the following. This implies that the case of a *parabolic* point $\mathbf{a}_0$ (or $\mathbf{b}_0$) is excluded. Later we briefly report on this case. According to (7), $A$ is represented with respect to $S$ by

$$\mathbf{a}(\phi(S)) = \begin{bmatrix} D^{-1} \cdot E \cdot S + O(x^2) \\ \frac{1}{2}S^\top \cdot E \cdot D^{-1} \cdot E \cdot S + O(x^3) \end{bmatrix}, \quad (8)$$

By letting $F = I + D^{-1} \cdot E$ the parametrization of the convolution surface $A \star B$ is

$$(\mathbf{a}+\mathbf{b})(S) = \begin{bmatrix} F \cdot S + O(x^2) \\ \frac{1}{2} S^\top \cdot E \cdot F \cdot S + O(x^3) \end{bmatrix}. \tag{9}$$

Analogously, $C = A \star B$ can be represented with respect to $U$. If $\mathbf{a}_0 + \mathbf{b}_0$ is a regular point of $C$, which means that $F$ is regular, $C$ can be represented as graph with help of the reparametrization

$$T = F \cdot S + O(x^2), \text{ or } S = F^{-1} \cdot T + O(x^2).$$

The local graph representation of $C$ at $\mathbf{a}_0 + \mathbf{b}_0$ is

$$(\mathbf{a}+\mathbf{b})(T) = \begin{bmatrix} T \\ \frac{1}{2} T^\top \cdot F^{-\top} \cdot E \cdot T + O(x^3) \end{bmatrix}, \text{ with } F^{-\top} = (F^\top)^{-1}. \tag{10}$$

As known from differential geometry, the principal curvatures of $A \star B$ are determined by the eigenvalues of $M = F^{-\top} \cdot E$ and the associated directions are its eigenvectors. Moreover, Gaussian and mean curvature of $A \star B$ are $\det(M)$ and $\operatorname{trace}(M)$, respectively.

### Regularity of the convolution

According to our approach the regularity of the convolution $C$ at $\mathbf{a}_0 + \mathbf{b}_0$ depends on the regularity of $F = I + D^{-1} \cdot E$. This is a certain simplification but gives already some insight to the problem. Thus we assume that $\operatorname{rk}(D) = 2$ which says that $\mathbf{a}_0$ is either an elliptic or hyperbolic point of $A$. If $\operatorname{rk}(E) = 2$ the same holds for $\mathbf{b}_0$ on $B$, otherwise $\mathbf{b}_0$ is a parabolic point ($\operatorname{rk}(E) = 1$) or flat($\operatorname{rk}(E) = 0$).

The normal curvatures $\kappa^A(\mathbf{v}), \kappa^B(\mathbf{v})$ in direction of the tangent vector $\mathbf{v}$ at $\mathbf{a}_0$ and $\mathbf{b}_0$ are given by

$$\kappa^A(\mathbf{v}) = \mathbf{v}^\top \cdot D \cdot \mathbf{v},\ \kappa^B(\mathbf{v}) = \mathbf{v}^\top \cdot E \cdot \mathbf{v},$$

since the coefficient matrices of the first fundamental form at the origin $\mathbf{a}_0 = \mathbf{b}_0$ are both $I = \operatorname{diag}(1,1)$. The investigation of the regularity of $C$ is based on the rank of $F$.

**rk**$(F) = 2$**:** The convolution $C$ is regular at $\mathbf{a}_0 + \mathbf{b}_0$. This point is either elliptic or hyperbolic if $\operatorname{rk}(E) = 2$ and parabolic or flat if $\operatorname{rk}(E) = 1$ or $\operatorname{rk}(E) = 0$, respectively.

**rk**$(F) = 1$**:** There exists a vector $\mathbf{v} \neq \mathbf{o} = (0,0)^\top$ with

$$F \cdot \mathbf{v} = \mathbf{o} = \mathbf{v} + D^{-1} \cdot E \cdot \mathbf{v}, \Longrightarrow -D \cdot \mathbf{v} = E \cdot \mathbf{v} \Longrightarrow -\kappa^A(\mathbf{v}) = \kappa^B(\mathbf{v}).$$

The convolution possesses a singular point at $\mathbf{a}_0 + \mathbf{b}_0$. We consider curves $l$ on $A$ through $\mathbf{a}_0$ and their corresponding curves (with respect to coinciding unit normal vectors) through $\mathbf{b}_0$. The image curves $l'$ on the convolution $C$ have all the same tangent vector determined by $\mathrm{im}(F)$ except curves $l$ whose tangent vector is determined by $\mathbf{v} = \ker(F)$. The latter ones are mapped to curves $l'$ with a singularity at $\mathbf{a}_0 + \mathbf{b}_0$.

**$\mathbf{rk}(F) = 0$:** For any vector $\mathbf{v}$ we have $F \cdot \mathbf{v} = \mathbf{o}$. Thus, all the normal curvatures of $A$ and $B$ at $\mathbf{a}_0$ and $\mathbf{b}_0$ satisfy $-\kappa^A(\mathbf{v}) = \kappa^B(\mathbf{v})$. The convolution $C$ possesses a singular point at $\mathbf{a}_0 + \mathbf{b}_0$ and all curves through that point have a singularity there.

We observe that the behaviour of $C$ can be quite complicated. If both surfaces $A$ and $B$ are parabolic at $\mathbf{a}_0$ and $\mathbf{b}_0$ the proposed reparametrization (7) fails to work and one would have to use another technique to compute a parametrization of $C = A \star B$. Nevertheless, this case typically occurs for a finite set of corresponding points. The convolution $C$ typically is regular at the considered point $\mathbf{a}_0 + \mathbf{b}_0$. If $\ker(\mathrm{D}) = \ker(\mathrm{E})$ then $\mathbf{a}_0 + \mathbf{b}_0$ is a parabolic point of $C$ otherwise ($\ker(\mathrm{D}) \neq \ker(\mathrm{E})$) $\mathbf{a}_0 + \mathbf{b}_0$ is a flat point of $C$.

### Convolution of paraboloids with parallel axes

By omitting the higher order terms in (6) one obtains the case of two paraboloids with parallel axes. Equation (9) shows that the convolution $A \star B$ of two paraboloids $A, B$ with parallel axes is again a paraboloid in case of regularity of $F$. The reparametrization (7) is linear and (10) is a graph representation of $A \star B$.

If $\mathrm{rk}(F) = 1$, this condition holds for all pairs of corresponding points $\mathbf{a}, \mathbf{b}$ and $A \star B$ consists of singular points only and degenerates to a curve, see Figure 3. The right hand side figure shows the indicatrices, the curvature diagrams of both surfaces. At any pair of corresponding points there exists a direction $\mathbf{v}$ with $\kappa^A(\mathbf{v}) = -\kappa^B(\mathbf{v})$. Since (9) is quadratic, the singular curve is a parabola.

If $\mathrm{rk}(F) = 0$, this condition is again true for all pairs of corresponding points and $A \star B$ degenerates to a point.

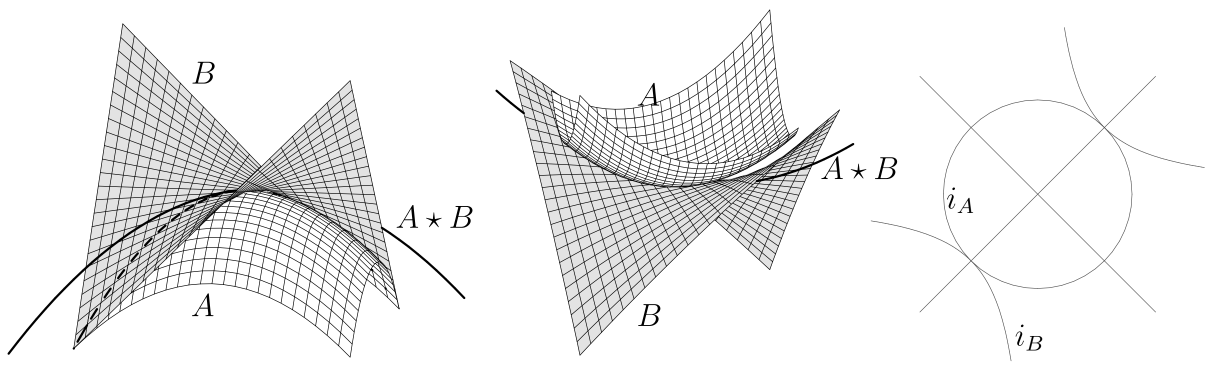


Figure 3: Left and middle: Degenerate cases of convolution 'surfaces'. Right: Curvature diagrams (indicatrices) of $A$ and $B$ at the origin.

# 4 Convolution of surfaces given by dense point clouds

We are given two oriented surfaces $A, B$ as sets of points $\mathbf{a}_i, i = 1, \ldots, M$ and $\mathbf{b}_j, j = 1, \ldots, N$ together with their associated oriented unit normal vectors $\mathbf{n}_a, \mathbf{n}_b$. For a moment we assume that $A, B$ are smooth surfaces and we will extent the construction to piecewise smooth surfaces later.

## 4.1 Computing corresponding points

Two points $\mathbf{a}$ and $\mathbf{b}$ are said to be *corresponding*, if $\mathbf{n}_a = \mathbf{n}_b$ holds. For any $\mathbf{a}$ there exists a set of corresponding points $\mathbf{b}_j$, which might be empty. Consequently, the convolution $A \star B$ is formed by points $\mathbf{c}_j = \mathbf{a} + \mathbf{b}_j$. Usually, this correspondence through equal normal vectors is not one-to-one. Obviously, the surface normal vector $\mathbf{n}_{c_j}$ of the convolution $A \star B$ at points $\mathbf{c}_j$ equals $\mathbf{n}_a$.

Figure 4 shows on the left hand side the construction of corresponding points of the convolution $A \star B$ of two planar curves $A, B$, and the one-parameter family of translated curves $\mathbf{b} + A$ on the right hand side. Figure 5 shows the point set of the convolution $A \star B$ of two planar curves $A, B$ on the left hand side and the extracted outer boundary $\Gamma$ of the outer envelope $A \star B$ on the right hand side.

In order to define the correspondence between $\mathbf{a} \in A$ and $\mathbf{b} \in B$ we proceed as follows: A point $\mathbf{a}$ with associated normal vector $\mathbf{n}_a$ is correpsonding to those $\mathbf{b}_j \in B$ whose normal

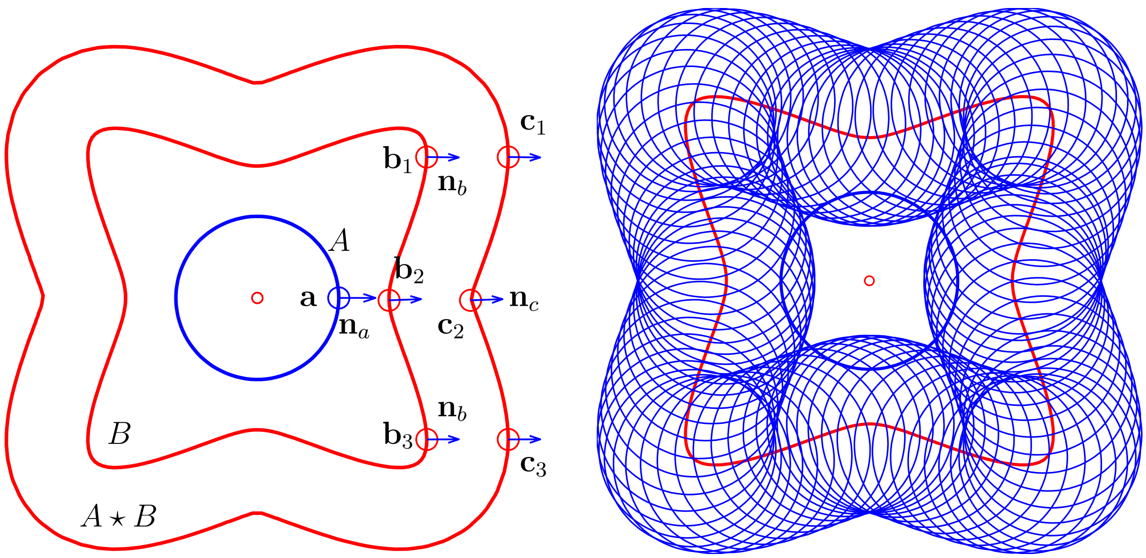


Figure 4: Corresponding points on $A$ and $B$ and family of translated curves $\mathbf{b} + A$

vectors $\mathbf{n}_{b_j}$ satisfy

$$\|\mathbf{n}_a - \mathbf{n}_{b_j}\| < \tau, \text{ or } \angle(\mathbf{n}_a, \mathbf{n}_{b_j}) < \tau. \tag{11}$$

These two requirements are almost equivalent for small values $\tau$. If the input surfaces $A$ and $B$ are given by rather *dense point clouds*, it is sufficient to define the correspondence by searching for nearest neighbors in the given sets of unit normal vectors $\mathbf{n}_a, \mathbf{n}_b$ according to (11). This does not require any triangulation of the input surfaces $A$ and $B$.

An alternative but more accurate construction uses triangulated input data and performs linear interpolation. It works as follows: Thus let $A$ and $B$ be given by data points $\mathbf{a}_i$ and $\mathbf{b}_j$, normal vectors $\mathbf{n}_a, \mathbf{n}_b$ and triangulations $S = \{s\}$ and $T = \{t\}$, respectively. We consider the set of triangles $\{t'\}$ whose vertices $\mathbf{n}_b$ are the unit normals of $B$ and let $\mathbf{a} \in A$ be a fixed point with unit normal $\mathbf{n}_a$. Let $t'$ be a triangle in the unit sphere $S^2$ with vertices $\mathbf{n}_{b_k}, k = 1, 2, 3$ which contains $\mathbf{n}_a$. Then, $\mathbf{n}_a$ can be represented by a convex combination $\sum \mathbf{n}_{b_k}\beta_k$, with $\beta_k > 0$. Normalizing these coefficients by $\sum \beta_k = 1$, they serve as barycentric coordinates with respect to the original triangle $t$ with vertices $\mathbf{b}_k$. Consequently, the point $\mathbf{b} = \sum \mathbf{b}_k\beta_k$ approximately corresponds to the given point $\mathbf{a}$. Performing this construction for each triangle $t'$ containing $\mathbf{n}_a$, one obtains all points $\mathbf{b}_j$ corresponding to the fixed given point $\mathbf{a}$. Finally, $\mathbf{c}_j = \mathbf{a} + \mathbf{b}_j$ are points of the convolution surface $A \star B$.

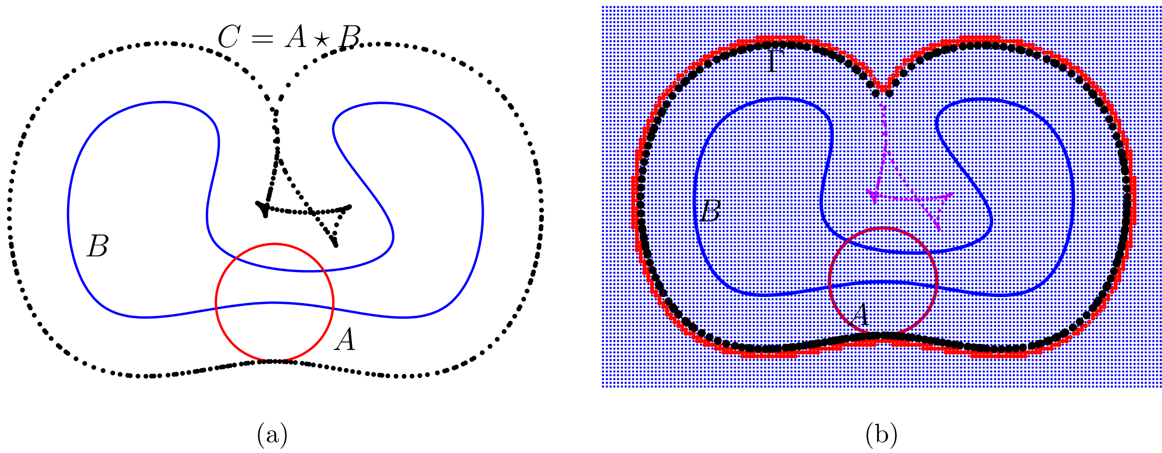


Figure 5: a) Envelope $C = A \star B$. b) Extaction of the outer boundary $\Gamma$.

## 4.2 Extracting the outer boundary from the convolution

So far we have computed an unorganized set of points $\mathbf{c}$ with associated unit normals $\mathbf{n}_c$ covering the convolution surface $C = A \star B$. Figure 5(a) shows that the envelope $C = A \star B$ might have global self-intersections and possess parts in the interior. We apply a global, grid-based method to extract the outer boundary $\Gamma$ from the envelope of $C$. Examples are illustrated in Figures 6 and 7.

The envelope $C$ is placed in a rectangular grid whose cell size is larger than $\delta$, the average point distance at the envelope. The unsigned distance function of $C$, evaluated at the grid points is computed. In order to trim those parts of $C$ lying in the interior of the outer boundary $\Gamma$ a marching method is performed, similar to that described in [20, 14].

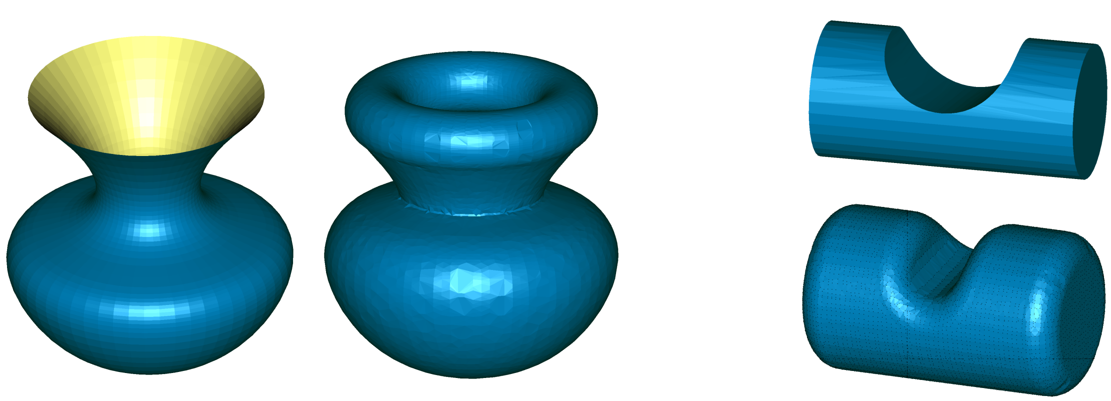

Figure 6: Objects and their offsets (at some distance) computed as Minkowski sum.

Applying this method results is a correct labeling of the grid points as *inside* or *outside*. Thus it defines in fact a *signed distance function* of the outer boundary $\Gamma$. By taking a small band of *outside* grid points, the outer boundary $\Gamma$ is defined as set of nearest neighbors of this small band (Figure 5(b)). This results in a relatively uniform sampling of $\Gamma$ by data points with associated unit normal vectors. The principle of the boundary extraction is illustrated in the 2D-Figure 5(b) and the method works analogously in 3D. The extraction of the outer boundary can be significantly accelerated by considering only those grid points within a certain bandwidth ($\sim 5\delta$) of the convolution $C$. self-intersections of the envelope are smoothed out and have to be treated separately (section 4.5).

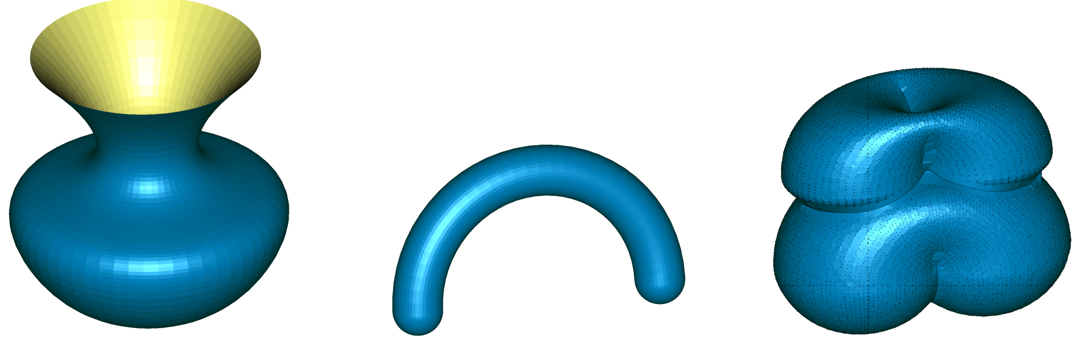

Figure 7: Left and middle: Objects $A$ and $B$. Right: Minkowski sum $A + B$.

## 4.3 Computing inner boundaries of the envelope

Even the simple two-dimensional examples in Figures 4 and 5 show that the convolution $C$ of two oriented objects $A$ and $B$ can possess one or more inner boundaries. We recall that the correspondence between $A, B$ is defined via coincidence of oriented unit normal vectors $\mathbf{n}_a, \mathbf{n}_b$. To determine potential points of the inner boundaries the orientation of $\mathbf{n}_a$ is reversed to $-\mathbf{n}_a$. Figure 8 shows the outer and inner envelopes with associated unit normal vectors (left and middle) and the outer and inner boundaries on the right hand side.

For extraction of the outer boundary the marching method requires a seed point being definitely outside the convolution. The active front stops at the outer boundary. When extracting the inner boundaries one proceeds similarly, but the seed point has to be contained in an inside region bounded by points whose normal vectors point inwards, see

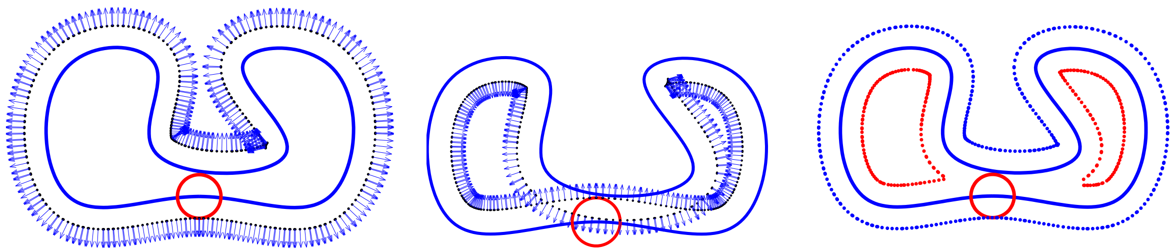

Figure 8: Outer (left) and inner (middle) envelope and extracted boundary points (left).

Figure 8 (middle). Finally, the extracted inner boundary points have to be partitioned into connected sets and each of these sets of points has to be triangulated. The figures illustrate the two-dimensional case only, but the procedure in 3D is analogous.

### 4.4 Edges and corners

Real world objects typically possess *edges* and *corner* and the envelope computation has to take this into account. For the practical implementation we assume that the edges of the objects $A, B$ can be reliably detected and fitted by curves determined by two different patches of the input surfaces locally. At an edge point $\mathbf{p}$ there exist two different unit normal vectors $\mathbf{n}_l$ and $\mathbf{n}_r$ with respect to both patches intersecting at this edge. We exclude curves of regression here. The set of unit normal vectors at $\mathbf{p}$ form a wedge spanned by $\mathbf{n}_l$ and $\mathbf{n}_r$. At a corner $\mathbf{p}$ the set of unit normal vectors is even two-dimensional and is defined by the convex cone of unit normals of the surface patches meeting at $\mathbf{p}$.

Since the set of relevant normals is larger at edges and corners, these points contribute usually more likely to the envelope. Thus it is important to detect sharp edges and corners at the objects to guarantee an accurate representation of the outer boundary.

Let $A$ be a piecewise smooth surface which contains edges and let $B$ be a smooth surface. We restrict our consideration to a single edge $c$ of $A$. Assume that $c$ is a smooth curve with parametrization $\mathbf{c}(t)$ and let the left hand and right hand side normal vector fields of $A$ along $\mathbf{c}(t)$ be denoted by $\mathbf{n}_l(t)$ and $\mathbf{n}_r(t)$. The contribution of the edge $c$ and surface $B$ to the outer boundary of the convolution $A \star B$ consists of that part of $\mathbf{c} + B$ which lies inside the wedge spanned by $\mathbf{n}_l(t), \mathbf{n}_r(t)$.

Figure 6 shows offsets of two CAD-models with precise edges and corners. These offsets are

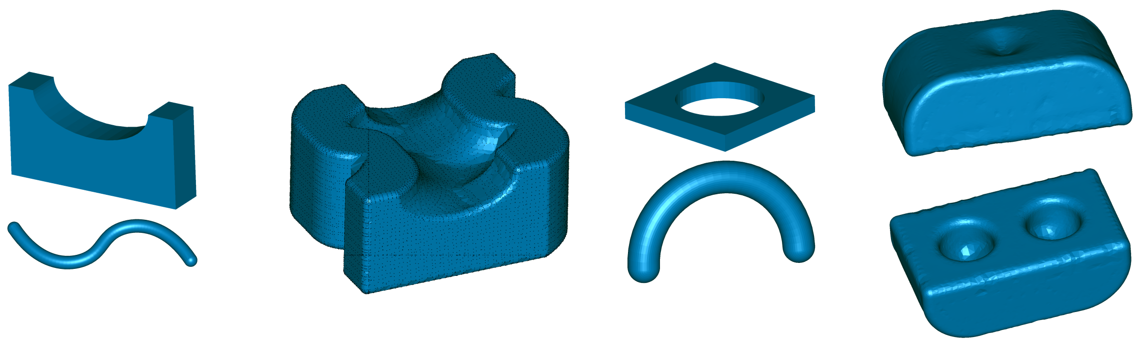

Figure 9: Left: CAD-model and pipe surface and their Minkowski sum. Right: Plate with hole and half torus and two views of their Minkowski sum.

computed as Minkowski sums of the objects and a sphere. Of course, for offset computation there exist simpler algorithms and it is not necessary to define a correspondence between the input surfaces. These examples have been chosen to illustrate the algorithm since in case of more complex input surfaces it is often hard to imagine how the Minkowski sum looks like.

### 4.5 Global self-intersections of the envelope

According to the nature of convolution surfaces, $A \star B$ as well as the outer boundary $\Gamma$ might possess global self-intersections. Let $\Gamma$ be covered by a point set $G$ whose normals are denoted by $\mathbf{n}_g$. Under the assumption that the smooth parts of $\Gamma$ are nearly uniformly sampled, global self-intersections can be detected with help of a *feature sensitive* metric (see [15]). Onces having detected these feature locations, the global self intersections are frequently reconstructed nicely by intersecting profile sections along the detected sharp feature ([14]). An example is displayed in Figure 10.

## 5 Conclusion

We have presented a method to compute the boundary surface of the Minkowski sum of two input objects which typically are piecewise smooth surfaces $A, B$. The method is based on envelope computation with respect to translations defined by $A$ or $B$ and a trimming procedure. The method applies to the representation of the outer boundary surface as well

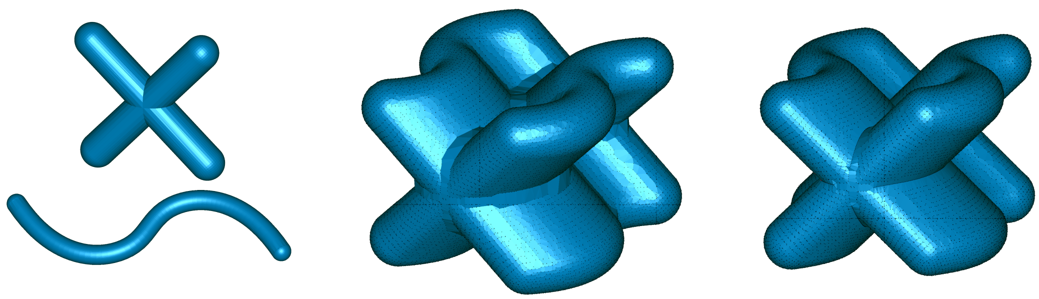

Figure 10: Minkowski sum of pipe surface and object. Right: Sharpened edges of the Minkowski sum.

as possibly occurring inner boundaries. Additionally we performed a local analysis of the envelope in dependence of the normal curvatures of the input surfaces.

The prototypical implementation has been performed in Matlab. The models are typically sampled by 2.5k to 10k data points. The computation takes usually less than 60 sec., including nearest neighbor searching, initialization and marching on the grid, extraction of outer boundary, etc., if the data structure of the models is already prepared.

The presented method of envelope computation applies not only to a two parameter family of translations but as well to a general two parameter family of motions whose rotational part is non trivial. Nevertheless, the translations are distinguished because the envelope is fully determined by the correspondence defined via the normal vector fields $\mathbf{n}_a$, $\mathbf{n}_b$ of the input surfaces $A, B$. This reduces the computational costs significantly compared to the effort of envelope computation in case of general motions.

**Acknowledgment.** This work has been carried out partially within the Kplus competence center *Advanced Computer Vision* and funded partially by the Austrian Science Fund FWF within the research network S92. The authors like to thank Helmut Pottmann and Boris Odehnal for helpful comments.

# References

[1] Bajaj, C. and Kim, M.-S. 1989. Generation of configuration space obstacles: The case of a moving algebraic curve, *Algorithmica* **4**(2), 157–172.

[2] Bloomenthal, J. and Shoemake, K., 1991. Convolution Surfaces, Computer Graphics, Vol. 25, No. 4, 251–256.

[3] Farin, G., Hoschek, J., and Kim, M.-S., 2002. *Handbook of Computer Aided Geometric Design*, Elsevier.

[4] Farouki, R.T., 2003. Minkowski combination of complex sets - Geometry, Algorithms and applications, in *Curve and Surface Design: Saint Malo 2002*, T. Lyche, M.-L. Mazure and L.L. Schumaker (eds.), Nashboro Press, 123–146.

[5] Halperin, D., 2002. Robust Geometric Computing in Motion, The international Journal of Robotics Research, Vol. 21, No. 3, pp.219–232.

[6] Kaul, A. and Farouki, R.T., 1995. Computing Minkowski sums of planar curves, *Int. J. of Computat. Geom. and Appl.* **5**, 413–432.

[7] Kohler, K. and Spreng, M., 1995. Fast Computation of the C-Space of Convex 2D Algebraic Objects, *The Int. J. of Robotics Research* **14**(6), 590-608.

[8] Lee, I.-K., Kim, M.-S. and Elber, G., 1998a. Polynomial/Rational Approximation of Minkowski Sum Boundary Curves, *Graphical Models* **60**, No.2, 136–165.

[9] Lee, I.K., Kim, M.-S. and Elber, G., 1998b. The Minkowski Sum of 2D Curved Objects, *Proceedings of Israel-Korea Bi-National Conference on New Themes in Computerized Geometrical Modeling*, Tel-Aviv University, 155-164.

[10] Mühlthaler, H. and Pottmann, H., 2003. Computing the Minkowski sum of ruled surfaces, *Graphical Models*, **65**, 369–384.

[11] Oeltze, S. and Preim, B., 2005, Visualization of Vasculature With Convolution Surfaces: Method, Validation and Evaluation, IEEE Transactions on Medical Imaging, Vol. 24, No.4, 540–548.

[12] O'Rourke, J., 1994: *Computational Geometry in C*, Cambridge University Press.

[13] Peternell, M. and Manhart, F., 2003. The convolution of a paraboloid and a parametrized surface, *Journal for Geometry and Graphics* **7**, 157-171.

[14] Peternell, M., Pottmann, H., Steiner, T. and Zhao, H., 2005: Swept Volumes, *Computer-Aided Design Appl.* **2**, pp. 599-608.

[15] Pottmann, H., Steiner, T., Hofer, M., Haider, C. and Hanbury, A., 2004. The isophotic metric and its application to feature sensitive morphology on surfaces, in: *Computer Vision — ECCV 2004, Part IV*, eds.: Pajdla, T. and Matas, J., Lecture Notes in Computer Science, Springer, **3024**, pp. 560–572.

[16] Sampoli, M.L., Peternell, M. and Jüttler, B., 2006. The convolution of a paraboloid and a parametrized surface, *Computer Aided Geometric Design* **23**, 179–192.

[17] Seong, J.-K., Kim, M.-S. and Sugihara, K., 2002. The Minkowski Sum of Two Simple Surfaces Generated by Slope-Monotone Closed Curves, *Proceedings of Geometric Modeling and Processing 2002*, Japan, 33–42.

[18] Sherstyuk, A., 1999. Convolution Surfaces in Computer Graphics. PhD thesis, Monash Univ., Australia.

[19] Varadhan, G. and Manocha, D., 2004. Accurate Minkowski Sum Approximation of Polyhedral Models, In *Pacific Conference on Computer Graphics and Applications*, IEEE Computer Society, pp. 392–401.

[20] Kim, Y.J.,Varadhan,G., Lin, M.C. and Manocha,D., 2004. Fast swept volume approximation of complex polyhedral models, *Computer Aided Design* **36**, pp. 1013–1027.

[21] Wallner, J. and Yang, Q., 2005. Swept volumes of many poses, Geometry Processing 2005, Symposium Proceedings, Eurographics/ACM SIGGRAPH, pp.161–170.